


Estimation of increased pulmonary wedge pressure by an algorithm based on noninvasively measured pulmonary diastolic pressure in cardiac patients independent of left ventricular ejection fraction

Paolo Barbier MD, FESC¹  | Cuono Cucco MD² | Marco Guglielmo MD³ |
Anca Simoniuc MD, PhD² | Iacopo Fabiani MD, PhD² | Nicola Riccardo Pugliese MD² |
Gabriele Savioli MD, PhD⁴ | Frank Lloyd Dini MD, FESC²

¹Imaging Department, Jilin Heart Hospital, Changchun, China

²Cardiovascular Diseases Unit 1, Cardiovascular and Thoracic Department, University of Pisa, Italy

³Centro Cardiologico Monzino, IRCCS, Milano, Italy

⁴Fondazione IRCCS Policlinico San Matteo, Emergency Department, University of Pavia, Italy

Correspondence

Paolo Barbier, MD, Imaging Department, Jilin Heart Hospital, #5558 Jingyue Road, Changchun 130117, Jilin Province, China.
Email: dr.barbier@jlheart.org

Abstract

Aim: Pulmonary artery diastolic pressure (PADP) correlates closely with pulmonary wedge pressure (PAWP); therefore, we sought to evaluate whether an algorithm based on PADP assessment by the Doppler pulmonary regurgitation (PR) end-diastolic gradient (PRG) may aid in estimating increased PAWP in cardiac patients with reduced or preserved left ventricular (LV) ejection fraction (EF).

Methods and Results: Right heart catheterization, with estimation of PAWP, right atrial pressure (RAP), PADP, and Doppler echocardiography, was carried out in 183 patients with coronary artery disease ($n = 63$), dilated cardiomyopathy ($n = 52$), or aortic stenosis ($n = 68$). One-hundred and seventeen patients had LV EF $< 50\%$. We measured the pressure gradients across the tricuspid and pulmonary valves from tricuspid regurgitation (TRV) and PR velocities. Doppler-estimated PADP (e-PADP) was obtained by adding the estimated RAP to PRG. An algorithm based on e-PADP to predict PAWP, that included TRV, left atrial volume index, and mitral E/A, was developed and validated in derivation ($n = 90$) and validation ($n = 93$) subgroups. Both invasive PADP ($r = .92, P < .001$) and e-PADP ($r = .72, P < .001$) correlated closely with PAWP, and e-PADP predicted PAWP (AUC: 0.85, CI: 0.79-0.91) with a 94% positive predictive value (PPV) and a 55% negative predictive value (NPV), after exclusion of five patients with precapillary pulmonary hypertension. The e-PADP-based algorithm predicted PAWP with higher accuracy (PPV = 94%; NPV = 67%; accuracy = 85%; kappa: 0.65, $P < .001$) than the ASE-EACVI 2016 recommendations (PPV = 97%; NPV = 47%; accuracy = 68% undetermined = 18.9%; kappa: 0.15, $P < .001$).

Conclusions: An algorithm based on noninvasively e-PADP can accurately predict increased PAWP in patients with cardiac disease and reduced or preserved LV EF.

KEYWORDS

Doppler echocardiography, pulmonary regurgitation, pulmonary wedge pressure

1 | INTRODUCTION

It has been demonstrated that the pulmonary valve regurgitation (PR) velocity profile correlates closely with pulmonary artery diastolic pressure (PADP)¹ and the latter with pulmonary artery wedge pressure (PAWP).² While PR is often of limited hemodynamic significance, the Doppler assessment of the pulmonary regurgitation end-diastolic pressure gradient (PRG) may offer a first approximate estimation of PAWP. Although dependent on pulmonary vascular resistance (PVR), inclusion of PRG as the starting point of an algorithm to estimate increased PAWP may offset the intrinsic limitations of standalone PR sampling and help overcome limitations of the recently proposed algorithms,³⁻⁵ including the need of a separate approach for patients with reduced or preserved left ventricular (LV) ejection fraction (EF), presence of unclassified cases, and the central role assigned to mitral annulus tissue Doppler measurements. Therefore, we aimed to develop and validate an algorithm based on noninvasively measured PADP (e-PADP: Doppler-estimated PADP) to predict increased PAWP in a prospective cohort of patients with heart disease and reduced or preserved LV EF undergoing cardiac catheterization.

2 | METHODS

2.1 | Study subjects

Diagnostic cardiac catheterization was prospectively carried out in 183 patients with coronary artery disease (n = 63), dilated cardiomyopathy (n = 52), or aortic stenosis (n = 68). An echo-Doppler examination was performed within one hour of cardiac catheterization. Reasons for exclusion were as follows: inadequate acoustic window (n = 17), atrial fibrillation or flutter (n = 30), severe organic mitral regurgitation (n = 16), more than moderate aortic regurgitation (n = 7), valve prosthesis (n = 3), mitral valvuloplasty (n = 2) or stenosis (n = 6), or congenital heart disease (n = 3). Elevated LV filling pressure (LVFP) was defined as PAWP >12 mm Hg.⁵ All patients were hemodynamically stable and on oral medical therapy. An algorithm to predict PAWP >12 mm Hg was developed in the first 90 patients (derivation group) and tested in the following 93 patients (validation group). The research protocol was approved by the Internal Review Board; all patients gave written informed consent.

2.2 | Echocardiography

Transthoracic echocardiography was performed with an Acuson Sequoia C256 (Mountain View) with a 3.5 MHz transducer. M-mode and two-dimensional measurements, including LV biplane indexed end-diastolic and end-systolic volumes and EF and biplane left atrial volume index (LAVi), were assessed. From the pulsed-Doppler mitral velocity tracings, the following measurements were made: E and A velocities, and E/A ratio; E-wave deceleration time. Doppler tissue

imaging longitudinal velocities were recorded with the sample volume placed at the junction between the septal and lateral LV wall and the mitral annulus in the 4-chamber view, and peak early myocardial wave (e'm) velocities were measured. The ratio of mitral E peak velocity and averaged e' velocity (E/e'm ratio) was calculated. Estimates of tricuspid regurgitation velocity (TRV) and PR velocity were recorded by continuous Doppler. The peak TRV was assigned as the average among five tricuspid regurgitation (TR) envelopes of greatest maximal velocities and spectral density. The peak PR flow velocity at end-diastole was averaged in the same way. In the case of poor velocity signals, TR or PR velocities were enhanced with contrast (agitated saline), as previously reported.^{6,7} Recordings were obtained at quietly held end-expiration, and measurements averaged over three consecutive beats by experienced operators (CC, AS), blinded to hemodynamic data. The pressure gradient across the tricuspid valve (TRG: trans-tricuspid pressure gradient) and PRG were measured using the simplified Bernoulli equation. The estimated pulmonary artery systolic pressure (PASP) and PADP (e-PADP) were calculated as the sum of the TRG, and PRG added to the estimated right atrial pressure (RAP) derived from the size and the inspiratory collapse of the inferior vena cava.⁶ Virtual basic coding (using Microsoft Excel™) with Boolean operators (that described the different diagnostic paths shown in Figure 1) was used to build two algorithms to predict increased PAWP: (a) A first algorithm was developed to estimate normal or increased PAWP based on the ASE-EACVI 2016 recommendations flowcharts, with a 2-step approach as recently outlined by Andersen et al⁵ for patients with structural heart disease and preserved or reduced LV EF (<50%). Variables included were as follows: EF, e'm, E/e'm, E/A, TRG, and LAVi. Patients with preserved LV EF (≥50%) and no structural heart disease were not included in our study (no indication for catheterization) (Figure 1, right panel). (b) A second simplified algorithm was based on e-PADP with a single-step approach (independently of EF) by adding TRG, mitral E/A, and LAVi with the aim to compensate for under- and overestimation of PAWP by e-PADP and maximize PAWP estimation accuracy (Figure 1, left panel).

Suggested methodology to record appropriately PR velocities (Supporting information online Data S1: Page 11; Figures S6 and S7; Movie S1-S3) and description of contrast-enhanced Doppler study (Supporting information online, Page 2) are available in the supporting information online Data S1.

2.3 | Cardiac catheterization

Pressure measurements were acquired using a Cournand end-hole catheter advanced through the right heart chambers into the pulmonary arteries. Specifically, the catheter was advanced into the upper, middle, and lower pulmonary arteries, and PAWP was measured and recorded in each position and averaged. All hemodynamic recordings were obtained at held quiet end-expiration. The pulmonary artery wedge position was confirmed by the appearance of a typical wedge pressure tracing. Mean PAWP was determined automatically by the

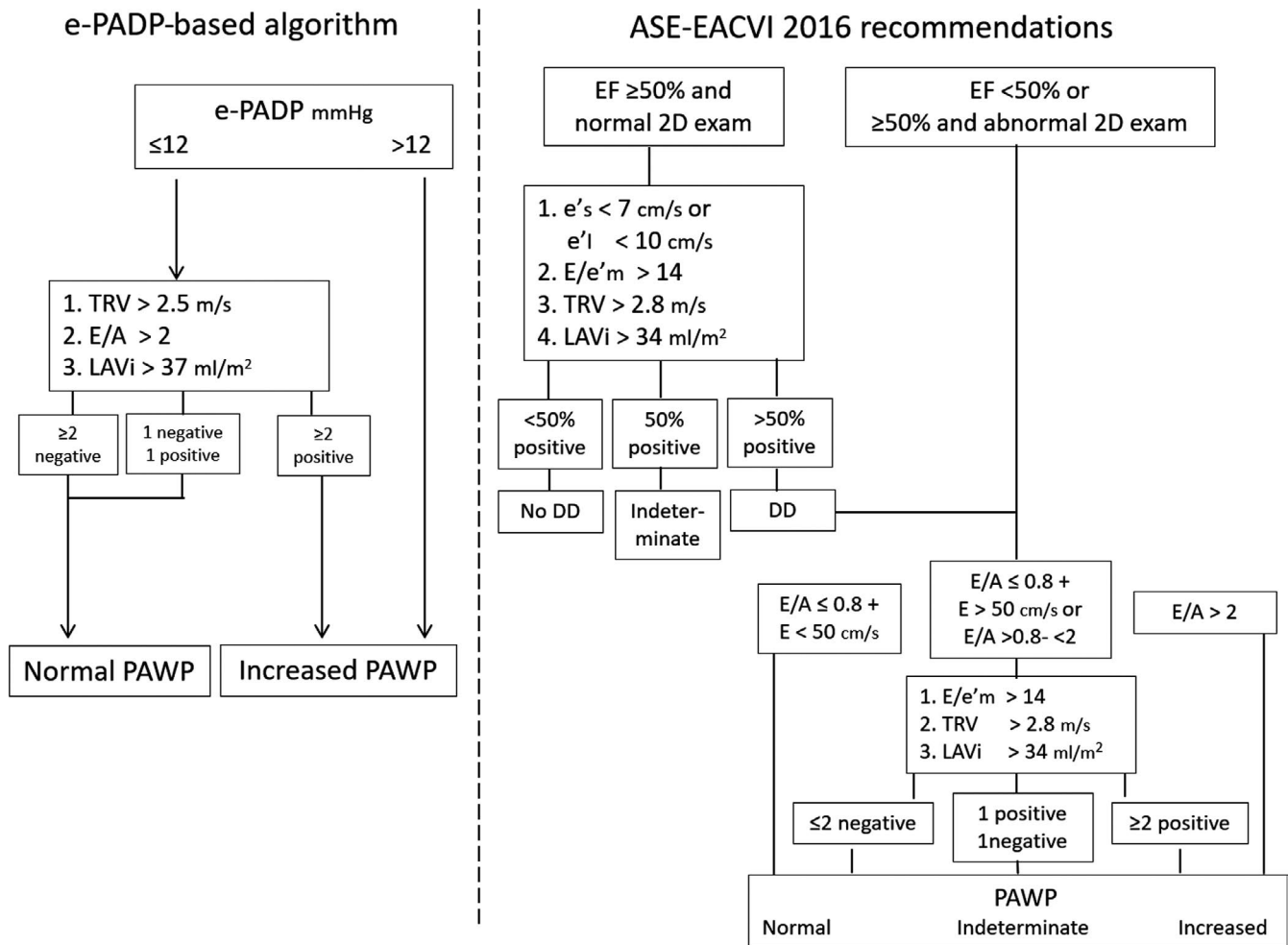


FIGURE 1 Comparison of the flowcharts for prediction of pulmonary artery wedge pressure: An algorithm based on the pulmonary artery end-diastolic pressure vs the ASE-EACVI 2016 algorithm. E = mitral peak E-wave velocity; e'l = tissue Doppler annular lateral peak early diastolic velocity; e's = tissue Doppler annular septal peak early diastolic velocity; E/e'm = mitral-to-myocardial early velocities; E/A = mitral peak E/A wave ratio; EF = ejection fraction; LAVi = left atrial maximum volume index; e-PADP = Doppler-estimated pulmonary artery diastolic pressure; PAWP = pulmonary artery wedge pressure, TRV = tricuspid regurgitation velocity

monitoring system (Horizon 9000 WS, Mennen Medical Ltd). RAP, PASP, PADP, mean pulmonary artery pressure, and PAWP were measured with a Hewlett-Packard transducer and a 7005 Marquette polygraph. Increased PAWP was defined as >12 mm Hg.⁵ Cardiac output was measured by the Fick method. PVR ($\text{dynes} \times \text{s} \times \text{cm}^{-5}$) was then calculated. Pulmonary hypertension was defined as mean pulmonary artery pressure ≥ 25 mm Hg, and elevated PVR was defined as ≥ 240 $\text{dynes} \times \text{s} \times \text{cm}^{-5}$; precapillary pulmonary artery hypertension (PAH) was defined as PVR ≥ 240 $\text{dynes} \times \text{s} \times \text{cm}^{-5}$ and PAWP ≤ 12 mm Hg.

2.4 | Statistical analysis

Continuous variables were expressed as mean \pm SD. All measurements were compared by standard parametric methods. Correlation analysis was performed by Spearman's correlation test. Multivariate regression analysis was used to determine the noninvasive predictors

of increased PAWP. Receiver operating characteristic (ROC) curve analysis was performed to determine the threshold values of e-PADP, and E/e'm for increased PAWP. Positive predictive value (PPV), negative predictive value (NPV), accuracy, and kappa statistic were used to assess the performance of e-PADP, and of the algorithms in estimating increased PAWP. Inter-observer reproducibility was assessed using mean percent of error (MPE, the absolute average difference between measurements divided by the mean value of the measurements $\times 100$). A *P* value $< .05$ was considered significant, and SPSS v.20 (IBM SPSS, Inc) was used.

3 | RESULTS

3.1 | Patients' characteristics

Patient characteristics and measurements are shown in Table 1 for both derivation and validation subgroups. Reduced LV EF ($<50\%$)

TABLE 1 Patients' characteristics, catheterization, and echocardiographic data for the derivation and validation groups

	Derivation group (range)	Validation group (range)
	n = 91	n = 92
Age (range) (y)	69 ± 11 (38–87)	67 ± 11 (39–87)
Sex (m:f)	60:35	56:32
BSA (m ²)	1.8 ± 0.17	1.8 ± 0.19
NYHA	2.4 ± 0.6	2.4 ± 0.7
Heart rate (bpm)	75 ± 15 (45–130)	76 ± 19 (40–175)
Right atrial pressure (mm Hg)	7 ± 3	7 ± 3
Pulmonary artery systolic pressure (mm Hg)	42 ± 11	43 ± 15
Pulmonary vascular resistances (dynes × s × cm ⁻⁵)	162 ± 86	170 ± 100
Pulmonary artery wedge pressure (mm Hg)	17 ± 7 ^a (5–34)	18 ± 8 ^b (8–45)
LV end-diastolic volume index (mL/m ²)	82 ± 27	81 ± 26
LV ejection fraction (%)	47 ± 15 (20–80)	44 ± 16 (15–80)
Left atrial volume index (mL/m ²)	46 ± 16	44 ± 13
Doppler pulmonary diastolic pressure (mm Hg)	14 ± 5	15 ± 6
Tricuspid peak systolic gradient (mm Hg)	33 ± 9	36 ± 11
Mitral E/A ratio	1.4 ± 1.3	1.4 ± 1.3
E/e'm	10 ± 3.7	11 ± 4.7

Note: Abbreviations: BSA = body surface area; E/e'm = mitral-to-myocardial early velocities; LV = left ventricular; NYHA = New York Heart Association.

^aMedian = 16.5 mm Hg.

^bMedian = 17 mm Hg.

was found in 117/183, and increased PAWP in 130/183 patients. Differences between patients with normal and increased PAWP are shown in Table S1. Contrast enhancement of Doppler signals of TR and PR were performed in 35% of patients with the achievement of optimal or near-optimal envelope tracings. In 22 patients (12.1%), PR could not be sampled, resulting in 87.9% feasibility of the method.

3.2 | Hemodynamic variables

Elevated PVR was observed in 25/183 patients and precapillary PAH in 5/183 patients: The latter were excluded from algorithm analysis. PADP correlated closely with PAWP in both patients with normal ($r = .92, P < .001$) or elevated PVR ($r = 0.86, P < .001$), but

overestimated PAWP in patients with precapillary PAH, as expected (Figure 2A); PASP correlated closely with PAWP ($r = .86, P < .001$).

3.3 | Relation between noninvasive variables and pulmonary artery pressures

Both TR and PR velocities closely correlated with pulmonary pressures and PAWP (Table S2). Among Doppler and two-dimensional variables, only e-PADP and TRG showed a good correlation with PAWP either in patients with reduced or preserved LV EF (Table S3). Correlations between e-PADP and PAWP were similar in patients with normal ($r = .65, P < .001$) or increased ($r = .74, P < .001$) PVR.

Bland-Altman plots of the overall correlation showed good accuracy (low bias), with fair limits of agreements, suggesting moderate precision (Figure S2). When patients were categorized according to a threshold of 12 mm Hg of invasive PAWP and e-PADP (Figure 2B), it emerged that 123 of them were correctly classified by e-PADP, whereas e-PADP underestimated PAWP in 30 patients, and overestimated it in 8 (4 of them with precapillary PAH). In contrast, E/e'm was useful to estimate increased PAWP only in cardiac patients with reduced LV EF (Figure S3A; single cutoff of 8 cm/s). In the overall study population, multiple regression analysis showed that PAWP was determined ($r = .88, r^2 = .77, P < .001$) by TRG ($B = 0.25, SE = 0.05$), e-PADP ($B = 0.36, SE = 0.09$), and E/e'm ($B = 0.3, SE = 0.09$).

At ROC analysis, PAWP >12 mm Hg was accurately identified by e-PADP (78%) independently of LV EF (Figure S4A). The exclusion of patients with elevated PVR did not modify the accuracy of the latter prediction model. In contrast, E/e'm (8.5 cutoff) well predicted PAWP only in patients with reduced LV EF (Figure S4B).

3.4 | The Algorithm Based on noninvasively measured pulmonary diastolic pressure

The Boolean analysis showed that the implementation of TRV, E/A, and LAVi in a model that comprised e-PADP maximized the ability to noninvasively recognize patients with increased PAWP (Figure 1; Table 2). Finally, Table 2 illustrates the performance of the algorithm based on e-PADP compared with the performance of standalone e-PADP and of the 2016 ASE-EACVI recommendations for the assessment of diastolic dysfunction. Compared with the ASE-EACVI 2016 recommendations, standalone e-PADP exhibited higher sensitivity and NPV, and accuracy was further increased by the introduction of our algorithm.

3.5 | Reproducibility

The MPE (mean ± SD) for PRG, TRV, E/A, e'm, and LAVi was, respectively, 8.7 ± 4.8%; 5.5 ± 5%; 4.5 ± 2.7%; 6.9 ± 4.7%; and 2.7 ± 2.1%.

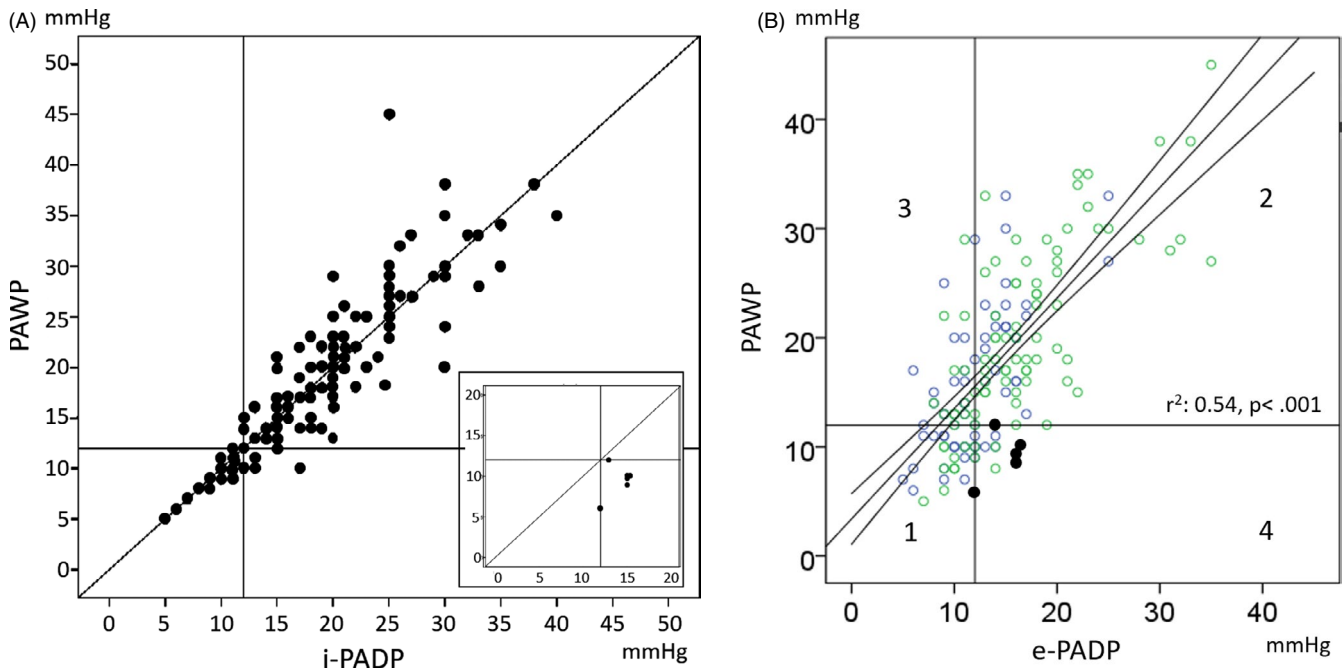


FIGURE 2 Relations with wedge pressure (PAWP) of pulmonary diastolic pressure (A, i-PADP) and Doppler-estimated pulmonary diastolic pressure (B, e-PADP) in the overall study population. A, Patients with normal pulmonary pressures and postcapillary (main chart, $n = 178$, $r = .91$, $P < .001$) or precapillary PAH (insert, $n = 5$, $r = .4$, $P = ns$). X and Y reference lines set at 12 mm Hg. B, On both axis: 12 mm Hg cutoffs: $r = .72$, $P < .001$. Blue circles: normal pulmonary vascular resistance ($PVR \leq 240 \times \text{dynes} \times \text{s} \times \text{cm}^{-5}$); green circles: increased PVR; black filled circles: precapillary PAH. Doppler echocardiography detects accurately normal (1) and increased PAWP (2), underestimates PAWP in 30 (3) and overestimates in 8 (4) patients, 3 of whom with precapillary PAH

4 | DISCUSSION

In this study, an algorithm to noninvasively predict PAWP, that comprised e-PADP, TRV, LAi, and mitral E/A, was developed and validated in patients with heart disease independently of LV EF. This approach resulted to be more accurate than the ASE/EACVI 2016 recommendations in predicting LVFP in patients without precapillary PAH or increased PVR.³

4.1 | Accuracy and reliability of hemodynamic pressure measurements

The 2016 recommendations emphasize the significance of estimating LVFP as the primary step in the assessment of LV diastolic function.³ The possibility to predict increased LVFP in stable patients with heart disease (independently of LV EF) is essential because this condition is related to poor outcomes and early echocardiography-guided treatment may reduce mortality.⁸

Cardiac catheterization studies have shown that PADP is usually equal to PAWP in most patients with LV failure, and thus, PADP can be used for clinical decision making instead of direct measurement of PAWP. If a precapillary component develops, the difference between PADP and PAWP increases, PADP will be higher than PAWP (out of proportion) and, therefore, a gradient becomes apparent between PADP and PAWP, and the latter will have to be measured to assess changes in LVFP.⁹

The calculated pressure difference between the pulmonary artery and the right ventricle in diastole added to the estimated RAP gives an estimate of PADP. A study of 200 patients demonstrated that a well-trained ultrasonographer or echocardiologist could achieve measurable e-PADP in 89% of patients.¹⁰ Despite recognition that noninvasive estimation of PAWP can be obtained from the assessment of PRG, this approach did not gain popularity because feasibility was considered too low ($\leq 60\%$).¹¹

Diagnosing LV diastolic dysfunction with echocardiography can be challenging. Four parameters have been recently introduced to determine diastolic dysfunction: an average (of septal and lateral) E/e'm >14 , a septal e'm <7 cm/c or lateral <10 cm/s, a TRV >2.8 m/s, and a LAVi >34 ml/m². If $<50\%$ of these parameters are present, the diastolic function is normal; if $>50\%$ there is diastolic dysfunction, and when parameters match ($=50\%$), diastolic function is indeterminate.³ Most of these echocardiographic indices are dependent on LV systolic function, mitral anatomy, and the effects of preload and several conditions can potentially hamper their accuracy in predicting elevated LVFP, including mitral valve disease, arrhythmias, pericardial constriction, LV segmental dysfunction, posteriorly directed aortic regurgitation, and heart transplantation.³⁻⁵

4.2 | Advantages of the algorithm approach

Although many echo-based algorithms have been proposed to estimate PAWP,¹²⁻¹⁴ none of them included the estimation of PADP. Our

TABLE 2 Performance of the algorithm based on the pulmonary artery end-diastolic pressure in comparison with the ASE-EACVI 2016 algorithm in estimating increased pulmonary artery wedge pressure

Patients	e-PADP	e-PADP	ASE-EACVI 2016	e-PADP	e-PADP
	All (n = 161) ^a	Without precapillary PAH (n = 156)	All (n = 183)	algorithm	algorithm
				All (n = 161) ^a	Without precapillary PAH (n = 156)
Unclassified (%)	0	0	19	0	0
Sensitivity (%)	74	74	57 ^b	86	85
Specificity (%)	82	88	96 ^b	78	86
Positive predictive value (%)	91	94	97 ^b	91	94
Negative predictive value (%)	55	55	47 ^b	69	67
Overall accuracy (%)	76	78	68 ^b	84	85
Kappa*	0.49	0.52	0.15	0.62	0.65

Note: Abbreviations: e-PADP = Doppler-estimated pulmonary artery diastolic pressure, PAH = pulmonary artery hypertension, PAWP = pulmonary artery wedge pressure.

^aTwenty two patients (12.1%) excluded because pulmonary regurgitation could not be sampled.

^bNot accounting for 19% of unclassified patients: of these, 3 (6%) had normal, and 17 (12.9%) elevated PAWP.

*P < .001 for all.

results showed that standalone assessment of e-PADP could reliably identify most patients with elevated PAWP (Table 2 and Figures 1 and S4A), because of its high positive predictive value (Table 2). Its accuracy was superior to that of standalone E/e'm, that is currently the most widely used single variable to assess LVFP¹²⁻¹⁵ (Table S6), as it is evident from the wide scatter pattern in the relationship between E/e'm and PAWP (Figure S3A). A recent meta-analysis did not support the use of E/e'm in patients with preserved EF.¹⁶ In patients with decompensated systolic heart failure, both baseline and directional changes of E/e'm did not correlate with PAWP.¹⁷ Of note, the accuracy of standalone e-PADP was also superior to the guideline approach (Table 2).

The main problem with standalone e-PADP that emerged from our results (Table 1) was that it was affected by a low NPV. However, the integration of e-PADP with other variables, that is, TRV, LAi, and mitral E/A, that are well known parameters that can predict elevated LVFP in many patients with heart disease,^{3,8,12-17} remarkably contributed to improve overall accuracy in identifying elevated PAWP. Particularly, the inclusion of TRV and E/A was able to counterbalance the tendency of e-PADP to underestimate PAWP (Figure 2B). TRV appears also useful in identifying patients with low PAWP (Figure S5, lower cutoff = 2.5 m/s). Finally, an 85% accuracy was reached by implementing LAVi.¹⁸

Similarly, a low NPV reduced the overall accuracy of the ASE-EACVI 2016 algorithm in our patient cohort. Although probably multifactorial, we believe that the main problem was the integration in this algorithm of E/e'm, since the cutoff >14 tends to underestimate PAWP in both patients with increased and normal EF (Figures S3A,B).

4.3 | Limitations

The algorithm based on e-PADP represents an alternative method that can be applied in selected patients in whom LVFP

estimation cannot be achieved by the ASE-EACVI 2016 algorithm. Nevertheless, its main limitation is the inapplicability in assessing PAWP if a significant precapillary component of PAH coexists.¹⁹ Therefore, the possibility of the e-PADP-based algorithm to identify elevated LVFP is restricted to patients with postcapillary PAH. Another limitation resides in the significant number of patients excluded because the acoustic window was not adequate or because they presented with atrial fibrillation or mitral valve disease. With respect to our findings, obtained at least partially with contrast enhancement, the true feasibility of PR sampling is probably less in clinical practice, but the introduction of more modern echocardiographic equipment may eventually overcome this limitation (Table S5).

Measurement of PR is limited by undersampling (Figure 2B, sector 3), and estimation of PAWP is dependent on the pressure continuity between the pulmonary artery and veins and is not feasible in the presence of increased, fixed PVR (currently measurable by Doppler echocardiography) and precapillary PAH. Of note, increased PVR per se was not a limiting factor in our patients (Table 2). Although the correlation of e-PADP with PAWP was fair, it was still not accurate enough to be used clinically (Figure 2). In this setting, ROC analysis identified a high PPV of e-PADP in predicting PAWP >12 mm Hg, although with a low NPV, thus suggesting the necessity to implement additional variables to increase accuracy.

4.4 | Conclusions

In patients with cardiac disease without precapillary PAH, an algorithm based on the acquisition of PR Doppler trace can accurately estimate elevated PAWP independently of LV EF, providing an advantage in NPV and accuracy over the ASE/EACVI 2016

recommendations. Nonetheless, our findings should be considered as preliminary, awaiting confirmation in a broader patient population and in patients excluded in the derivation cohort (mitral valve disease, atrial fibrillation).

CONFLICT OF INTERESTS

The authors report no relationships that could be construed as a conflict of interest.

AUTHOR CONTRIBUTIONS

Concept/design: P. Barbier, FL Dini involved in concept/design of the manuscript. Data analysis/interpretation: P. Barbier, M. Guglielmo, A. Simioniuc, I. Fabiani, NR Pugliese, FL Dini involved in data analysis/interpretation. Drafting article: P. Barbier, M Guglielmo, FL Dini involved in drafting article. Critical revision of article and approval: P. Barbier, FL Dini involved in critical revision of article and approval. Statistics: P. Barbier, G. Savioli involved in statistics. Data collection: P. Barbier, FL Dini, Simioniuc, I. Fabiani, NR Pugliese, G. Savioli involved in data collection.

ORCID

Paolo Barbier  <https://orcid.org/0000-0001-9242-5011>

REFERENCES

- Masuyama T, Kodama K, Kitabatake A, et al. Continuous-wave Doppler echocardiographic detection of pulmonary regurgitation and its application to noninvasive estimation of pulmonary artery pressure. *Circulation*. 1986;74:484–492.
- Jenkins BS, Bradley RD, Branthwaite MA. Evaluation of pulmonary arterial end-diastolic pressure as an indirect estimate of left atrial mean pressure. *Circulation*. 1970;42:75–78.
- Nagueh SF, Smiseth OA, Appleton CP, et al. Recommendations for the evaluation of left ventricular diastolic function by echocardiography: an update from the American Society of Echocardiography and the European Association of Cardiovascular Imaging. *Eur Heart J Cardiovasc Imaging*. 2016;12:1321–1360.
- Lancellotti P, Galderisi M, Edvardsen T, et al. Echo-Doppler estimation of left ventricular filling pressure: results of the multicentre EACVI Euro-Filling study. *Eur Heart J Cardiovasc Imaging*. 2017;18:961–968.
- Andersen OS, Smiseth OA, Dokainish H, et al. Estimating Left Ventricular Filling Pressure by Echocardiography. *J Am Coll Cardiol*. 2017;69:1937–1948.
- Pepi M, Tamborini G, Galli C, et al. A new formula for echo-Doppler estimation of right ventricular systolic pressure. *J Am Soc Echocardiogr*. 1994;7:20–26.
- Dini FL, Traversi E, Franchini M, Micheli G, Cobelli F, Pozzoli M. Contrast-enhanced Doppler hemodynamics for noninvasive assessment of patients with chronic heart failure and left ventricular dysfunction. *J Am Soc Echocardiogr*. 2003;16:124–131.
- Ponikowski P, Voors AA, Anker SD, et al. 2016 ESC Guidelines for the diagnosis and treatment of acute and chronic heart failure: The Task Force for the diagnosis and treatment of acute and chronic heart failure of the European Society of Cardiology (ESC) Developed with the special contribution of the Heart Failure Association (HFA) of the ESC. *Eur Heart J*. 2016;37:2129–2200.
- Vachieri JL, Adir Y, Barbera JA, et al. Pulmonary hypertension due to left heart diseases. *J Am Coll Cardiol*. 2013;62(25 Suppl):D100–D108.
- Borgeson DD, Seward JB, Miller FA Jr, et al. Frequency of Doppler measurable pulmonary artery pressures. *J Am Soc Echocardiogr*. 1996;9:832–837.
- Lee RT, Lord CP, Plappert T, et al. Prospective Doppler echocardiographic evaluation of pulmonary artery diastolic pressure in the medical intensive care unit. *Am J Cardiol*. 1989;64:1366–1370.
- Dini FL, Ballo P, Badano L, et al. Validation of an echo-Doppler decision model to predict left ventricular filling pressure in patients with heart failure independently of ejection fraction. *Eur J Echocardiogr*. 2010;11:703–710.
- Rafique AM, Phan A, Tehrani F, et al. Transthoracic echocardiographic parameters in the estimation of pulmonary capillary wedge pressure in patients with present or previous heart failure. *Am J Cardiol*. 2012;110:689–694.
- Ritzema JL, Richards AM, Crozier IG, et al. Serial Doppler echocardiography and tissue Doppler imaging in the detection of elevated directly measured left atrial pressure in ambulant subjects with chronic heart failure. *JACC Cardiovasc Imaging*. 2011;4:927–934.
- Santos M, Rivero J, McCullough SD, et al. E/e' ratio in patients with unexplained dyspnea: lack of accuracy in estimating left ventricular filling pressure. *Circ Heart Fail*. 2015;8:749–756.
- Sharifov OF, Schiros CG, Aban I, et al. Diagnostic accuracy of tissue Doppler index E/e' for evaluating left ventricular filling pressure and diastolic dysfunction/heart failure with preserved ejection fraction: a systematic review and meta-analysis. *J Am Heart Assoc*. 2016;5:e002530.
- Mullens W, Borowski AG, Curtin RJ, et al. Tissue Doppler imaging in the estimation of intracardiac filling pressure in decompensated patients with advanced systolic heart failure. *Circulation*. 2009;119:62–70.
- Tsang SM, Barnes ME, Gersh BJ, et al. Left atrial volume as a morphophysiological expression of left ventricular diastolic dysfunction and relation to cardiovascular risk burden. *Am J Cardiol*. 2002;90:1284–1289.
- Guazzi M, Naeije R. Pulmonary hypertension in heart failure: pathophysiology, pathobiology, and emerging clinical perspectives. *J Am Coll Cardiol*. 2017;69:1718–1734.

SUPPORTING INFORMATION

Additional supporting information may be found online in the Supporting Information section.

Data S1. Further material related to correlations between PAWP and Doppler echocardiographic variables, and practical implementation of e-PADP.

Figure S1. A, mitral valve flow velocities, normal PAWP; B, mitral valve flow velocities, elevated PAWP; C, pulmonary regurgitation end-diastolic velocity (0.65 m/s), normal PAWP; D, pulmonary regurgitation end-diastolic velocity (1.6 m/s), elevated PAWP; E, pulsed Doppler tissue velocities, lateral mitral annulus; F, pulsed Doppler tissue velocities, septal mitral annulus; G, pulmonary regurgitation end-diastolic velocities, with saline contrast. a': pulsed tissue Doppler peak late diastolic velocity; A, mitral peak A wave velocity; e' = pulsed tissue Doppler peak early diastolic velocity; E, mitral peak E wave velocity; PAWP = pulmonary wedge pressure; s' = pulsed tissue Doppler peak systolic velocity. The white arrow points at pulmonary regurgitation end-diastolic velocity

Figure S2A. Bland and Altman analysis plot assessing the correlation between PAWP and PADP: bias = -0.1 mm Hg, 95% limits of agreement = 6.2 to -6.4 mm Hg

Figure S2B. Bland and Altman analysis plot assessing the correlation between PAWP and e-PADP: bias = -3.5 mm Hg, 95% limits of agreement =7 to -14 mm Hg

Figure S3A. Relation between pulmonary artery wedge pressure (PAWP) and E/e'm (mitral peak E wave/mean tissue Doppler e') in patients with reduced (< 50%; $r = .58$, $P < .001$) ejection fraction. Patients with E/e'm >15 have increased PAWP, whereas most patients in the 8-15 range and half of the patients with E/e'm <8 have increased PAWP.[15]

Figure S3B. Relation between pulmonary artery wedge pressure (PAWP) and E/e'm (mitral peak E wave/mean tissue Doppler e') in patients with normal ($\geq 50\%$; $r = .36$, $P = .004$) ejection fraction. As in patients with reduced ejection fraction (Figure S3A) patients with E/e'm >15 have increased PAWP, whereas most patients in the 8-15 range and half of the patients with E/e'm <8 have increased PAWP. [15]

Figure S4A. ROC analysis for Doppler pulmonary diastolic pressure (e-PADP) excluding 5 patients with precapillary pulmonary hypertension. State = pulmonary artery wedge pressure (PAWP) and test = e-PADP variables (both cutoffs = 12 mm Hg). Black line: all ejection fractions (EF), AUC = 0.85 (95% CI = 0.79-0.91), $P < .001$; sensitivity = 74%; specificity = 88%. Red line: reduced EF, AUC = 0.82 (95% CI = 0.74-0.91), $P < .001$; sensitivity = 73%; specificity = 84%. Blue line, normal EF, AUC = 0.89 (95% CI = 0.81-0.97), $P < .001$; sensitivity = 77%; specificity = 91%.

Figure S4B. ROC analysis for E/e'm in all patients. Black line: all patients, with state variable = PAWP (cutoff = 12 mm Hg), and test variable = E/e'm (mitral peak E wave/ mean tissue Doppler e' ratio), AUC = 0.77 (95% CI = 0.69-0.84), $P < .001$, with 71% sensitivity and 72% specificity using E/e'm cutoff = 8.5. Red line: patients with reduced EF, AUC = 0.85 (95% CI = 0.77-0.92), $P < .001$, with 77% sensitivity and 77% specificity using a E/e'm cutoff = 8.5. Blue line: patients with normal EF, AUC = 0.5 (95% CI = 0.35-0.65), $P = ns$.

Figure S5. Relations of pulmonary artery wedge pressure (PAWP) with: the tricuspid valve regurgitation peak systolic velocity/ gradient (TRV/ TRG); mitral E/A; left atrial maximum volume index (LAVi). All y reference lines set at 12 mm Hg. TRV/ TRG: values below 2.5 m/s /25 mm Hg and above 3.2 m/s/ 40 mm Hg identify respectively normal and increased PAWP, whereas intermediate values are unrelated to PAWP. E/A: the relation with PAWP is quadratic (logarithmic x axis), and above the cutoff = 2, E/A identifies increased PAWP. In contrast, no relation exists between LAVi and PAWP. Blue circles: normal pulmonary vascular resistance ($PVR \leq 240$ 103 dynes $\times s \times cm^{-5}$); green circles: increased PVR.

Figure S6. Examples of 2D and color Doppler visualization of pulmonary valve and pulmonary regurgitation. A, Short axis of the base centered on the aortic root. B, Short axis of the base centered on the pulmonary artery. C, trace pulmonary regurgitation, central jet. D, trace pulmonary regurgitation, medial commissural jet. E, mild

pulmonary regurgitation, central jet. F, trace pulmonary regurgitation, lateral commissural jet. Ao = aortic root; PA = pulmonary artery; PR = pulmonary regurgitation; PV = pulmonary valve; RVOT = right ventricular outflow tract.

Figure S7. Examples of continuous wave Doppler tracings of pulmonary regurgitation velocities (without use of contrast). 1A: Variability of end-diastolic velocity during quiet respiration; 1B: Stable end-diastolic velocity, at held end-expiration; 2A: sub-optimal recording secondary to suboptimal visualization of pulmonary regurgitant jet (Movie S1); 2B: optimal end-diastolic velocity recording secondary to modification of scan line alignment with regurgitant jet (Movie S2); 3: Pulmonary regurgitation with 2 regurgitant jets, minimal central and mild commissural (posterior): optimal alignment of continuous wave scan line with the commissural jet (Movie S3); 4. Visualization limited to enddiastolic velocity may be sufficient if the notch caused by atrial contraction (secondary to increase in right ventricular end-diastolic pressure) is recorded; 5A: Optimal alignment of Doppler scan line with central pulmonary regurgitant jet; 5B: Optimal visualization of the pulmonary regurgitant velocity profile; the end-diastolic atrial contraction notch is missing secondary to atrial stunning (post electrical cardioversion of atrial fibrillation). White arrow points at pulmonary regurgitation end-diastolic velocity; long dashed arrow points at atrial contraction notch.

Movie S1. Color Doppler short axis of the base, optimized for pulmonary valve (transducer rotated towards patient's left shoulder): sub-optimal visualization of pulmonary regurgitant jet at posterior commissure (white arrow, between right and left pulmonary cusps). AV = aortic valve; PA = pulmonary artery; PV = pulmonary valve; RVOT = right ventricular outflow tract.

Movie S2. Increased quality of pulmonary regurgitant jet visualization (white arrow) - compared to Movie S1 - following slight anterior tilt of the transducer. AV = aortic valve; PA = pulmonary artery; PV = pulmonary valve; RVOT = right ventricular outflow tract.

Movie S3. Pulmonary regurgitation with two regurgitant jets, minimal central (small white arrow) and mild commissural (posterior; white arrow): the anterior direction of the jet originating posteriorly allows optimal alignment of the scan line. AV = aortic valve; PA = pulmonary artery; PV = pulmonary valve; RVOT = right ventricular outflow tract.

How to cite this article: Barbier P, Cucco C, Guglielmo M, et al. Estimation of increased pulmonary wedge pressure by an algorithm based on noninvasively measured pulmonary diastolic pressure in cardiac patients independent of left ventricular ejection fraction. *Echocardiography*. 2020;00:1-8. <https://doi.org/10.1111/echo.14581>